Theor Chem Acc (2010) 127:561–571
DOI 10.1007/s00214-010-0747-1

REGULAR ARTICLE

Theoretical study of proton-catalyzed hydrolytic deamination mechanism of adenine

Huanjie Wang · Fancui Meng

Received: 26 November 2009 / Accepted: 19 March 2010 / Published online: 6 April 2010

Abstract Water-assisted proton-catalyzed hydrolytic deamination of adenine to produce hypoxanthine has been studied using density functional theory method. Because adenine could be protonated at N1, N3, N7 and N10, four pathways initiated from the four different protonated adenines have been investigated. The first step of the four pathways is the nucleophilic attack of water with an assistant water to form a tetrahedral structure complex, and this is the rate-determining step. Including solvent effects decreased the relative energies of stationary points but have little effect on the structures. Pathway A is preferred due to the lowest energy barrier, and the relative free energy is 28.9 kcal/mol in vacuo. The outcomes show that adenine deamination under acidic condition is much easier to occur than under neutral condition due to lower energy barriers. The total atomic charge of C5 in the initial intermediate is correlated with the ease of deamination reaction. The more positive C5 atom is, the easier the deamination reaction is.

Keywords Adenine deamination · B3LYP · IEFPCM · Proton catalyzed

Electronic supplementary material The online version of this article (doi:10.1007/s00214-010-0747-1) contains supplementary material, which is available to authorized users.

H. Wang
School of Chemistry and Chemical Engineering, Shandong University, 250100 Jinan, People's Republic of China

F. Meng (✉)
Tianjin Institute of Pharmaceutical Research, 300193 Tianjin, People's Republic of China
e-mail: fancuimeng@yahoo.com.cn

1 Introduction

Base deamination can alter its hydrogen-bonding pattern, and this change to bases could change the mRNA codon identity and therefore induce synthesis of variant protein structure. For example, deamination of adenine results in the formation of hypoxanthine, and the latter selectively base pairs with cytosine instead of thymine. Thus, the original A–T base pair transforms into C–G base pair in the following transcription step. This mispairing when propagated is deleterious to the genome and could lead to cancer or cell death if unrepaired [1]. Spontaneous base deamination does not occur readily under normal physiological conditions.

The mechanisms of base deamination under neutral, basic and acidic conditions have been proposed several decades ago, although the exact mechanism is still unclear. Almatarneh et al. have studied the deamination reaction of cytosine under both neutral and basic environments [2, 3]. They found that the energy barrier of cytosine deamination with $2H_2O/OH^-$ agrees well with the experimental value. Labet et al. have also studied the deamination of cytosine with water and they hold that the tautomerization of cytosine or assistance of water is necessary for the deamination [4]. Very recently, they also studied the proton-catalyzed hydrolytic deamination mechanism of cytosine and 1-methylcytosine [5, 6], the obtained mechanism has a lower barrier than the OH^--catalyzed mechanism and lies closer to the experimental barrier. Similarly, the hydrolytic deamination mechanism of adenine with one or more water molecules has been elucidated [7–9] and the preferred pathway is through a tetrahedral complex formation.

Adenine, cytosine and guanine can deaminate during the hydrolysis of nucleic acids under strongly acidic conditions [10]. The study of acid-catalyzed hydrolytic deamination of

nucleic acids can provide useful insight into the degradation of nucleic acids, and elucidating the intrinsic reaction mechanism of nucleobases can improve our understanding of mutagenic processes. To our knowledge, proton-catalyzed cytosine deamination has been studied extensively [5, 6, 11], while no theoretical investigation on adenine deamination under acid mediates has been reported. Thus, in this paper, the deamination mechanism of adenine based on acid (H^+) catalysis has been investigated.

2 Calculation method

All the stationary points including reactants, transition states, intermediates and products have been optimized using density functional method B3LYP [12, 13] at 6-311G(d,p) level [14, 15]. Frequency analysis has been performed on all the stationary points to verify whether the obtained structures are transition structures or local minima.

IRC (Intrinsic Reaction Coordinate) calculations have been carried out from each transition state to ensure that the obtained transition state connected the right reactants and products. Single-point calculations at B3LYP/6-311G(d,p) level have been carried out on the previously optimized geometries obtained by the IRC procedure to get the variation of energy, reaction force and total atomic charge along the IRC. The reaction force [16] is defined as $F(\xi) = -\mathrm{d}E(\xi)/\mathrm{d}\xi$ and represents the force acting on the system to bring the reactants into the products. It has been used successfully for many systems [4, 17].

It has been found in many cases that solvent effect significantly influences the structure, stability, spectroscopy and other properties of DNA base [18–20]. Therefore, the obtained stationary points have been further optimized using IEF-PCM (polarized continuum model in the integral equation formalism) [21] method at B3LYP/6-311G(d,p) level, with the dielectric constant 78.39 to simulate the aqueous environment. The cavity was built using the united atom topologic model applied on the atomic radii of the UFF force field [22] and the default cavity was modified by adding individual spheres on hydrogen atoms linked to nitrogen and oxygen atoms by the keyword SPHEREONH.

To test the accuracy of B3LYP/6-311G(d,p) method, we also calculated all the optimized stationary points in solution using G3MP2//B3LYP/6-311G(d,p) methods. G3MP2//B3LYP [23, 24] method is a composite scheme based on the three single-point energies, i.e., QCISD(T)/6-31G(d) [25], MP2/6-31G(d) [26] and MP2/G3MP2large. The ZPVE corrections obtained by B3LYP/6-311G(d,p) method are used without scaling due to the fact that it agrees well with experimental values [27]. All calculations have been carried out using Gaussian03 software package [28].

3 Results and discussion

Protonation of nucleic acid bases plays a crucial role in many biochemical reactions, such as mutagenic processes, enzymatic reactions, stabilization of DNA triplex and other higher order structures [29]. The protonation of nucleic acid bases has been studied extensively using both experimental and theoretical approaches. Wu and McMahon [30] have studied the protonated adenine with ammonia and they found that the three different protonated adenine species has similar energies.

In this study, adenines protonated at N1, N7, N3 and N10 sites are taken as the initial reactants to study the deamination mechanism to convert adenine to hypoxanthine. Figure 1 is the schematic outline of the four pathways. Figures 2, 3, 4 and 5 are the optimized stationary structures along pathway A, B, C and D, respectively. Figure 6 is the free energy evolution along various pathways. The energies emerged in the following content refer to the relative free energies otherwise specified. Relative energies are listed in Table 1.

3.1 Deamination mechanisms

3.1.1 Deamination mechanisms in gas phase

3.1.1.1 Pathway A from N1 protonated adenine From Fig. 2, we can see that adenine protonated at N1 site forms a complex (Int1A) with two water molecules, in which three hydrogen bonds exist. This complex is −5.7 kcal/mol more stable than the sum of monomers (see Fig. 6a). The oxygen atom of first water molecule lies 2.978 Å from the C6 atom. The second water molecule creates two hydrogen bonds, one is N10–H15…O19, and the other is N7…H20–O19. The hydrogen bond distance between the N10 proton and the oxygen atom of the first water molecule is 1.800 Å and that between the N7 atom and hydrogen atom of water molecule is 1.993 Å. With the approaching of the first water to C6 atom and the elongation of O16–H17 bond, transition state TS12A is formed. In TS12A, the bond distances of C6…O16, O16…H17, H17…O19 are 1.634, 1.178 and 1.248 Å, respectively. The relative free energy of TS12A is 28.9 kcal/mol. Int2A is a complex of a tetrahedral structure with water obtained through TS12A, in which the hydroxyl group connects to C6 atom and the hydrogen atom of the second water transfers to N7 atom. There are two hydrogen bonds in Int2A with a relative free energy of 13.8 kcal/mol.

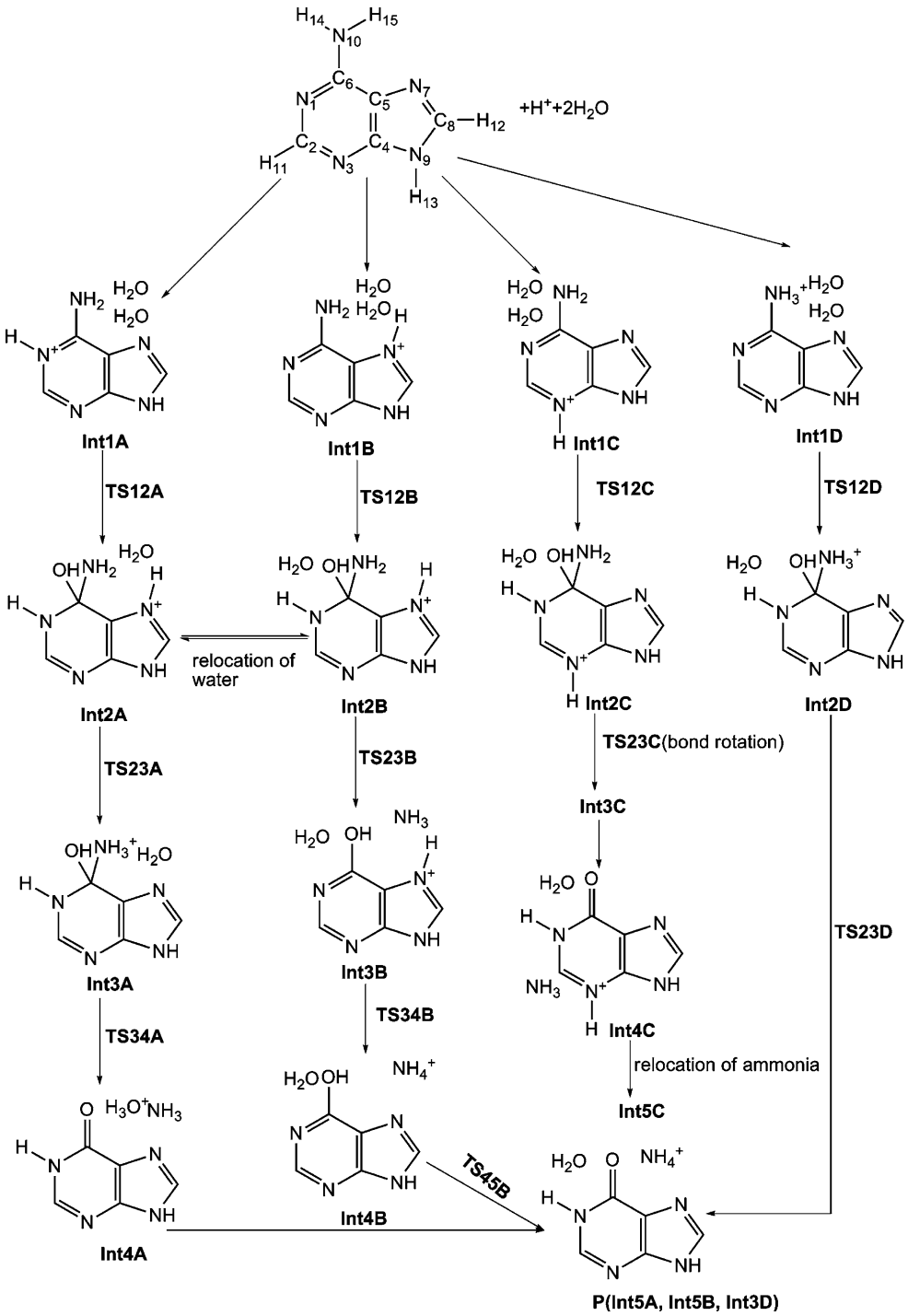

Fig. 1 Schematic outline of pathways for proton-catalyzed adenine deamination

In TS23A, the water molecule acts as a proton shuttle to transfer the hydrogen of N7 to amino nitrogen and the C6–N10 bond increases to produce ammonia. The relative energy of this transition state is 21.0 kcal/mol. Int3A is the intermediate obtained from TS23A, in which the N10…H17 distance is reduced to 1.079 Å, indicating the formation of ammonia.

TS34A is the transition state connecting Int3A and Int4A. The C6–N10 bond distance is 1.559 Å in Int3A while it is 1.585 Å in TS34A, indicating the bond cleavage of C6–N10. The vibration mode of TS34A according to the imaginary frequency is the rotation of the hydroxyl group. The hydrogen atom of the hydroxyl group rotates toward the oxygen atom of water and creates a hydrogen bond in

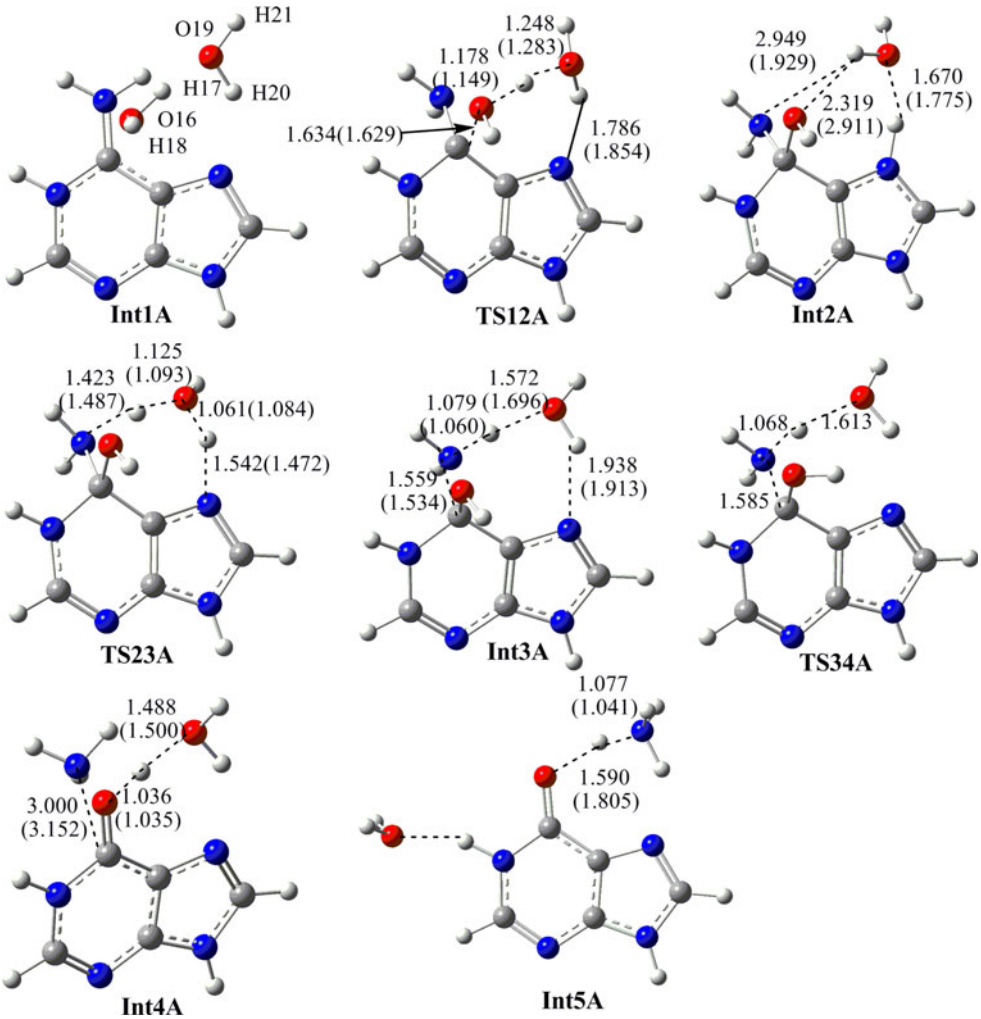

Fig. 2 Optimized stationary structures along pathway A. Bond distances (Å) both in gas phase and in solution phase (*in brackets*) are indicated

Int4A. The C6–N10 bond distance is 3.000 Å in Int4A, suggesting the release of ammonia molecule. Int4A is a complex of hypoxanthine…NH_3…H_3O^+, and it could be transformed to the complex hypoxanthine…NH_4^+…H_2O (Int5A), and the latter is much more stable than the former.

3.1.1.2 Pathway B from N7-protonated adenine The oxygen of the first water forms two hydrogen bonds with protonated adenine in the initial complex Int1B. In the transition state (TS12B), the two water molecules form a six-member ring structure with N1, C6, the two oxygen atoms and the two hydrogen atoms of the water molecules (Fig. 3). The second water acts as a proton shuttle in TS12B, transferring one of its protons to N1 atom. TS12B has a relative free energy of 39.7 kcal/mol. In2B is a complex of a tetrahedral structure with water obtained through TS12B, in which the hydroxyl group creates bond with C6 atom and the hydrogen atom of the second water transfers to N1 atom. Int2B is the same as Int2A except the position of water molecule.

With the approaching of the water to amino group, Int2B takes place a transition state TS23B. TS23B is also a six-member ring structure, in which the hydrogen atom bonded to N1 transfers to oxygen atom of water and the hydrogen atom of water transfers to amino group to release ammonia. From Table 1, one can see that the energy barrier of TS23B is lower than that of TS12B. Int3B is the intermediate obtained through TS23B, which is a complex of enol-type hypoxanthine protonated at position 7 with H_2O and NH_3. TS34B and TS45B are about hydrogen transfer and their energy barriers are much lower compared with the initial two transition states. TS34B is the transition state in which hydrogen of N7 transfers to NH_3 to create NH_4^+. TS45B is the transition state to cause enol–keto-type tautomerization of hypoxanthine with the help of water molecule. Int5B is the final complex of hypoxanthine with H_2O and NH_4^+ and it is −30.6 kcal/mol more stable than the reactants.

3.1.1.3 Pathway C from N3-protonated adenine In this mechanism, the adenine is firstly protonated at N3 position.

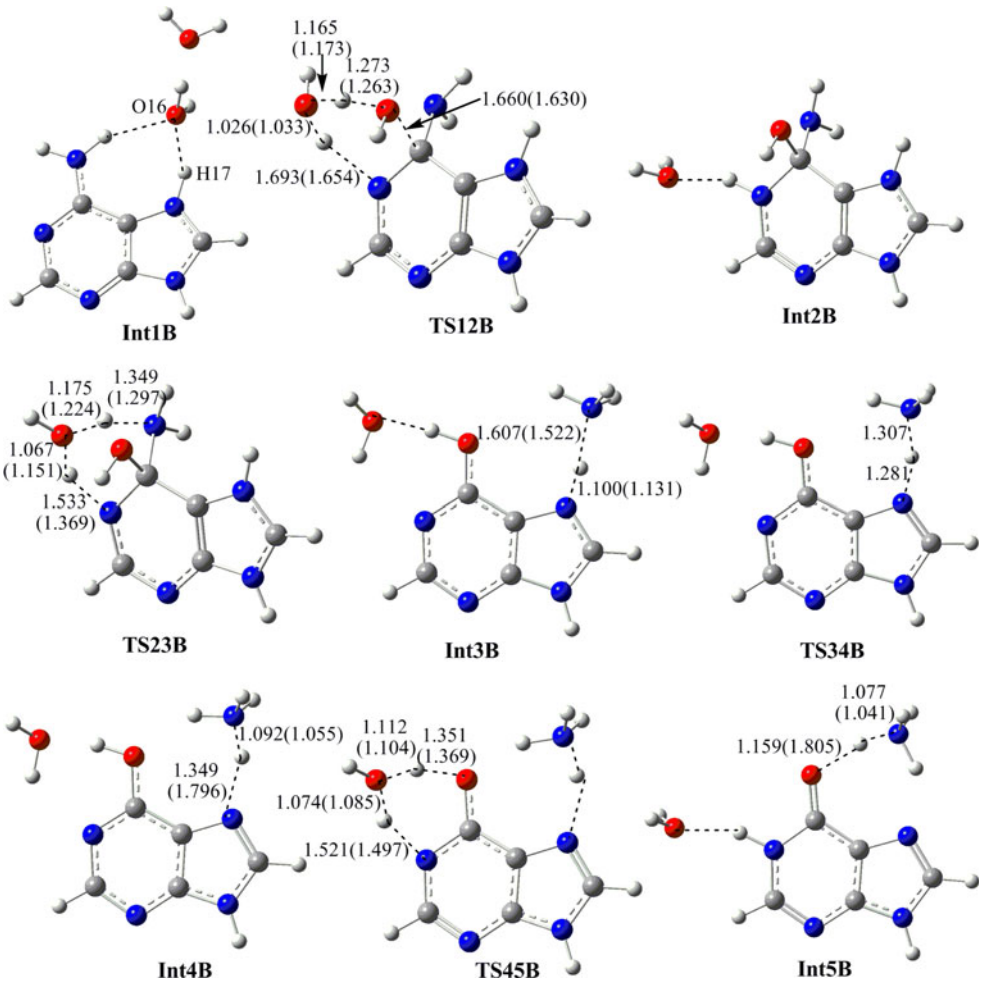

Fig. 3 Optimized stationary structures along pathway B. Bond distances (Å) both in gas phase and in solution phase (*in brackets*) are indicated

The optimized stationary structures of this pathway are shown in Fig. 4. One of the two water molecules lies 2.974 Å above C6 atom and the other water molecule is 2.438 Å away from N1 atom. Like TS12B, transition state TS12C also undergoes a six-member ring structure formed by the two water molecules and N1, C6 atoms. The relative free energy of TS12C is 39.0 kcal/mol. Int2C is the intermediate obtained from TS12C and it is 18.5 kcal/mol higher than the reactants. Int2C is also a tetrahedral structure with water.

TS23C is the transition state connecting Int2C and Int3C, which is about the rotation of the hydroxyl group and has a low free energy barrier of 5.0 kcal/mol as expected. The hydroxyl group rotates from toward the ring to toward the amino group through TS23C, which facilitates the hydrogen transfer from O atom of hydroxyl group to N10 atom. TS34C is the transition state where the hydrogen transfer occurred. The relative energy of TS34C is 39.5 kcal/mol. In TS34C, the water molecule acts as a shuttle to transfer the hydrogen atom of hydroxyl group to amino group. Then, the ammonia molecule leaves and the protonated adenine changes to protonated hypoxanthine.

Int4C is the intermediate obtained through TS34C and it can be transformed to Int5C, in the latter, the nitrogen atom of ammonia forms hydrogen bond with protonated N3. Int5C is −8.5 kcal/mol more stable than Int4C. Although a proton transfer from N3 to NH_3 seems possible and energetically favorable, no transition state was found.

3.1.1.4 Pathway D from N10-protonated adenine In this pathway, the initial intermediate is a hydrogen-bonded complex of adenine protonated at N10 with two water molecules. The hydrogen bond between N10 proton and the first water molecule is 1.406 Å and that between the two water molecules is 1.694 Å. In TS12D, the two water molecules form a six-member ring structure with N1 and C6 atoms. The distance between the hydroxyl group and C6 atom is 1.706 Å and distance between hydrogen atom and N1 atom is 1.570 Å. The relative free energy of TS12D is 31.8 kcal/mol. Int2D is the intermediate obtained through TS12D, which is also a complex of tetrahedral structure with water. The water molecule creates two hydrogen bonds in Int2D, one with proton of N10 (O…H bond 1.820 Å) and the other with proton of N1 (O…H bond 2.313 Å).

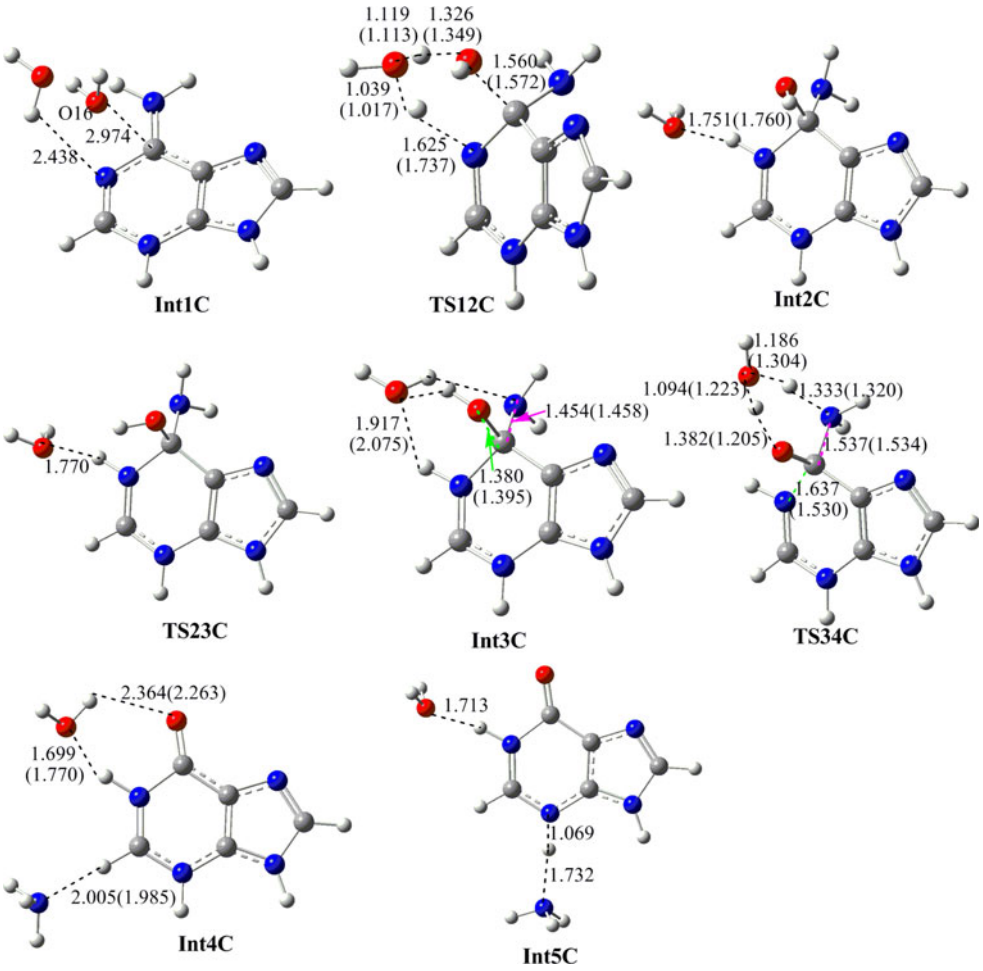

Fig. 4 Optimized stationary structures along pathway C. Bond distances (Å) both in gas phase and in solution phase (*in brackets*) are indicated

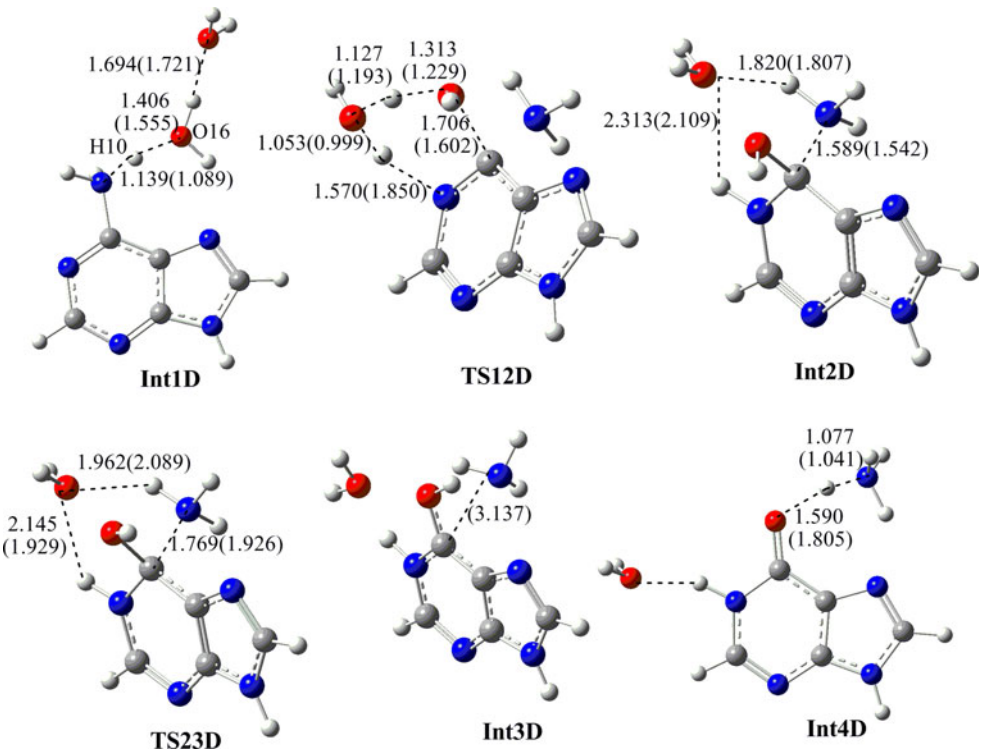

Fig. 5 Optimized stationary structures along pathway D. Bond distances (Å) both in gas phase and in solution phase (*in brackets*) are indicated

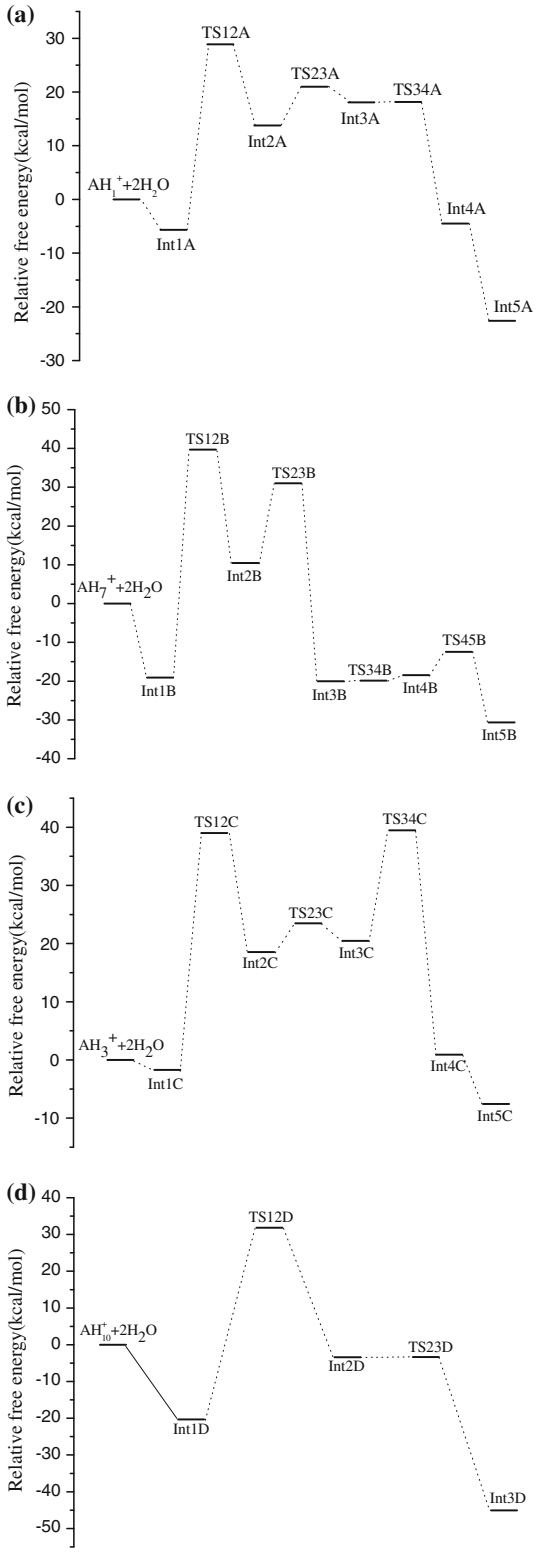

Fig. 6 Reaction pathway for the deamination of protonated adenine with $2H_2O$: **a** pathway A; **b** pathway B; **c** pathway C and **d** pathway D. Relative free energies are calculated at B3LYP/6-311G(d,p) level in gas phase

Then, NH_3 can leave through a simple transition state TS23D, in which the C6–N10 bond increases to 1.769 Å. TS23D has a very low energy barrier. The two hydrogen bonds are retained, while one is increased and the other is shortened. Int3D is the product obtained through TS23D. In Int3D, the hydrogen atom of hydroxyl group transfers to NH_3 to produce hypoxanthine…NH_4^+…H_2O complex. Int3D is −45.1 kcal/mol more stable than the reactants.

Pathway A, B and D produce the same final complex, hypoxanthine…NH_4^+…H_2O, while the final complex of pathway C is protonated hypoxanthine with H_2O and NH_3.

3.1.2 Deamination mechanism in aqueous solution

In order to investigate the solvent effects for adenine deamination mechanism, further geometry optimization has been performed using IEFPCM method. The selected bond distances are also shown in Figs. 2, 3, 4 and 5, respectively.

As for pathway A, the selected bond distances of TS12A change little when compared with those in gas phase. However, the hydrogen bonds are different for Int2A. H17 forms hydrogen bond with N10 atom instead of O16 atom. The geometries of TS23A and Int3A in solution are like those in gas phase. TS34A could not be obtained when including solvent effects. Bond distances in Int4A vary little in solution when compared with those in gas phase. The hydrogen atom is far from carboxyl oxygen atom in Int5A than in gas phase.

From Fig. 3, we can see that the optimized geometries of pathway B in solution are similar with those in gas phase. The transition state of TS34B does not exist in solution. But the hydrogen atom in Int4B forms a long bond distance with N7 atom than in gas phase. The same happens as to the hydrogen bond involving O16 atom in Int5B.

The position of the two water molecules in Int1C is different with that of gas phase. In solution, one of water molecules forms a cyclic structure with N1 and N10–H, while the other water molecule forms hydrogen bonds with the first water molecule. From Fig. 4, we can see that the geometries of TS12C and Int2C in solution vary little when compared with those in gas phase. The transition state TS23C about bond rotation of hydroxyl group could not been obtained in solution. Int3C is almost the same as that in gas phase. The "H_3O^+" character of O19 atom in TS34C weakened in solution when compared with that in gas phase. The structure of Int4C changed a little in solution. Int5C cannot be obtained in solution.

Table 1 Relative energies and relative free energies of various adenine deamination pathways under acidic circumstance (kcal/mol)

System	In vacuo			In aqueous solution			
	ΔE^{v}	ΔE^{v}_{ZPVE}	ΔG^{v}	ΔE^{s}	ΔE^{s}_{ZPVE}	ΔG^{s}	ΔE^{s}_{G3MP2}
Pathway A							
AH_1^++2H_2O	0.0	0.0	0.0	0.0	0.0	0.0	0.0
Int1A	−27.7	−23.0	−5.7	−20.2	−17.1	−22.4	−11.4
TS12A	5.5	9.1	28.9	14.2	16.3	10.7	14.0
Int2A	−10.6	−4.8	13.8	−7.4	−2.7	−11.2	−2.9
TS23A	−3.0	1.0	21.0	11.0	14.7	8.6	6.1
Int3A	−7.2	−1.0	18.1	3.9	10.6	2.1	4.0
TS34A	−6.8	−1.1	18.1	–	–	–	–
Int4A	−25.5	−21.3	−4.5	−6.9	−3.5	−7.7	−14.4
Int5A	−53.3	−48.0	−30.6	−29.2	−24.3	−30.4	−29.0
Pathway B							
AH_7^++2H_2O	0.0	0.0	0.0	0.0	0.0	0.0	0.0
Int1B	−40.2	−35.5	−19.1	−21.8	−17.6	−23.3	−26.1
TS12B	16.4	19.9	39.7	32.0	35.0	29.7	25.9
Int2B	−12.7	−7.1	10.5	−3.4	0.8	−5.3	−5.5
TS23B	7.5	11.1	31.0	22.1	24.5	19.9	17.3
Int3B	−41.3	−37.1	−20.0	−19.8	−16.7	−21.0	−26.5
TS34B	−40.4	−37.8	−19.9	–	–	–	–
Int4B	−41.8	−36.5	−18.4	−25.6	−20.0	−27.8	−25.8
TS45B	−34.9	−31.8	−12.4	−16.8	−14.0	−19.8	−19.7
Int5B	−53.3	−48.0	−30.6	−33.8	−28.5	−35.0	−37.2
Pathway C							
AH_3^++2H_2O	0.0	0.0	0.0	0.0	0.0	0.0	0.0
Int1C	−22.3	−18.2	−1.7	−12.5	−8.6	−13.6	−6.2
TS12C	17.5	20.1	39.0	28.3	31.5	25.8	26.5
Int2C	−3.5	1.5	18.5	8.1	13.6	8.1	4.2
TS23C	1.6	6.2	23.5	–	–	–	–
Int3C	−4.8	1.5	20.5	5.8	12.4	3.2	4.4
TS34C	17.7	20.2	39.5	23.3	25.7	20.6	30.0
Int4C	−18.0	−14.5	0.9	−13.4	−10.6	−15.0	−3.8
Int5C	−26.0	−22.4	−7.6	–	–	–	–
Pathway D							
AH_{10}^++2H_2O	0.0	0.0	0.0	0.0	0.0	0.0	0.0
Int1D	−40.5	−37.2	−20.3	−26.4	−23.9	−29.4	−27.0
TS12D	9.6	12.1	31.8	9.3	9.3	3.9	21.5
Int2D	−28.1	−22.2	−3.4	−10.5	−4.7	−12.2	−16.0
TS23D	−27.6	−22.5	−3.3	−8.9	−5.6	−11.0	−15.9
Int3D’	–	–	–	−16.4	−14.0	−16.2	−30.6
Int3D	−67.5	−62.8	−45.1	−45.7	−41.3	−47.1	−50.1

ΔE^{v}, relative energies in vacuo; ΔE^{v}_{ZPVE}, relative energies with ZPVE correction in vacuo; ΔG^{v}, relative thermal free energies in vacuo; ΔE^{s}, relative energies in solution; ΔE^{s}_{ZPVE}, relative energies with ZPVE correction in solution; ΔG^{s}, relative free energies in solution; ΔE^{s}_{G3MP2}, relative energies at G3MP2//B3LYP/6-311G(d,p) level

The selected bond distances shown in Fig. 5 indicate that as for pathway D, considering solvent effects does not change the geometries of stationary points much. Int3D’ is the complex of protonated enol form hypoxanthine with water and ammonia. Int3D’ can transform to hypoxanthine with water and ammonia cation through hydrogen transfer.

Including solvent effect decreased the relative free energies of the stationary points for the four pathways (see Table 1). However, the variational trends of free energies are similar with those in gas phase. From the aforementioned, we can see that including solvent effects has little effect on the deamination mechanism of protonated adenine. The structures and energetic properties change little when compared with the corresponding stationary points in gas phase. So in the following contents, we compare the four pathways in gas phase only.

3.1.3 *Effects of dispersion energy*

Although B3LYP has been successfully used for many biological systems [31–33], it cannot describe some weak interactions correctly due to its failure for dispersion interactions. In order to clear out whether the dispersion interaction is important for our system, G3MP2//B3LYP method was used due to the fact that it could give reliable energetic properties [2, 3]. From Table 1, one can see that the energy differences for the reaction between B3LYP and G3MP2 methods are no more than 10 kcal/mol except for Int1A, int3D and TS12D. So we can see that although B3LYP is able to predicate the geometry correctly, it is not good to predict the reaction energy barriers [34]. However, due to the reason that G3MP2 could not be used to calculate large system, B3LYP method is still an alternative method to give useful information.

3.2 Comparison of the four pathways

3.2.1 *Activation energies*

From Fig. 6, we can see that the first step of the tetrahedral intermediate formation is the determining step for the four pathways. Pathway A has the lowest energy barrier while pathway B has the highest one. The energy barrier of neutral hydrolytic adenine deamination according to the initial complex is 45.1 kcal/mol (ZPVE corrected energy at B3LYP/6-311G(d,p) level) for pathway a [9], while the corresponding energy barrier for pathway A of proton catalyzed adenine deamination is only 32.1 kcal/mol. Although proton catalysis decreases the energy barrier of adenine deamination reaction, the calculated activation energy barrier is still a high energy barrier to overcome, which is inconsistent with reference [10] that adenine could be deaminated under strongly acid conditions. Since adenine could be protonated at N1, N7, N3 and N10 sites, it may be multiply protonated instead of singly protonated under strongly acidic conditions and multiply protonation may decrease the activation energy of deamination.

3.2.2 *Reaction force evolution of the first step of the four pathways*

As is well known, the reaction force of an elementary step has a minimum and a maximum at the two inflection points of potential energy, and the reaction force vanishes at the transition state [4]. Figure 7a is the reaction force evolution of the first step of pathway A. The reaction force vanishes at the transition state, but it presents both a local minimum before the global minimum and a local maximum before the global maximum. This indicates that this step is a composition of two events and it is their simultaneity that causes only one energy barrier and one unique transition state [4]. The reaction force of pathway D (see Fig. 7d) also has local minimum and local maximum as pathway A, but the intensity is smaller than pathway A. This suggests that the simultaneity of pathway D is better than pathway A. The reaction force evolution of pathway B and C is alike to some extent. The activation part is less deep and wider than the relaxation part. The product region (after the maximum) of pathway B and C looks alike in terms of shape and intensity, which is due to the similar intermediates obtained through pathway B and C. Int2B and Int2C are almost the same except the position of the proton. Int2B is protonated at N7 while Int2C is protonated at N3. The transition states of the two pathways are alike and do not involve the protonated atoms, which results the similar product region of pathways B and C.

For pathways B, C and D, the first reaction steps all involve two hydrogen transfers: one from O16 to O19, and the other one from O19 to cyclic N1 of adenine. The transition states are all six-membered ring structures and O19 demonstrates more of "H_3O^+" character. However, this is not the case for pathway A. Pathway A also includes two hydrogen transfers, but the second hydrogen transferred is not to the cyclic N1 of adenine, but to the cyclic N7 of adenine. At the same time, the transition state of pathway A is a seven-membered ring structure and the hydrogen of water is far from the cyclic N7 atom. Owning to the longer distance between O19 and N7, the simultaneity of pathway A is worse than that of the other pathways, which further results the local minimum and maximum occurred in reaction force of pathway A.

3.2.3 *Total atomic charge evolution of the first step of the four pathways*

Figure 8a shows the evolution of the total atomic charge on C5 of the first step of various pathways. From Fig. 8a, one can see that C5 of pathway A has the most positive charge at the initial reactants while that of pathway D has the smallest charge. C5 is the adenine atom where nucleophilic attack occurs. The atomic charge on C5 decreases with the

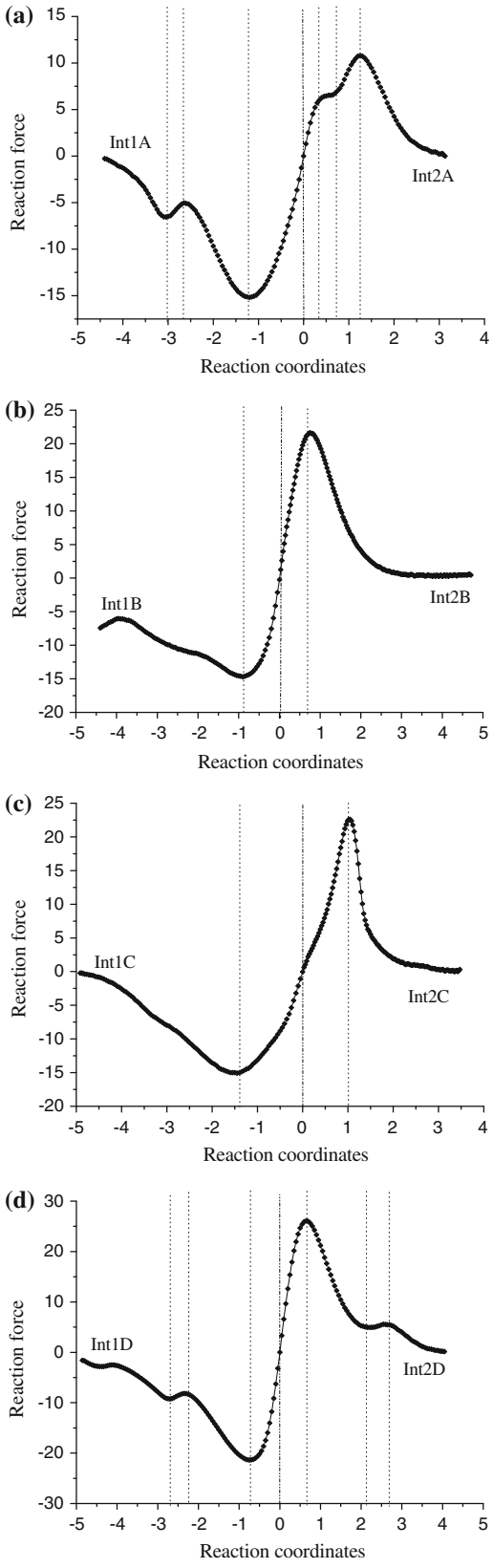

Fig. 7 Reaction force (corresponding to an energy in kcal/mol) along the reaction coordinates. The *dotted line* represents the position of transition state, local minimum or local maximum

approaching of hydroxyl group of water. The energy barrier height of the first transition state correlated with the total atomic charge on C5. The more positive charge C5 has, the lower the energy barrier of TS12 is, and the easier the nucleophilic attack takes place. Then, we can see that pathway A is the most possible pathway. With the creating of the C5–O16 bond, the charge of C5 increases gradually. However, due to the larger steric effect of ammonia than amino group, the C5–O16 and C5–N10 bond distances of pathway D are longer than those of the other three pathways. This may explain why the total atomic charge on C5 of pathway D is different from the other three pathways.

Figure 8b presents the evolution of the total atomic charge on O16 of the first step of the four pathways. From Fig. 8b, we can see that the trends of the total atomic charge on O16 are almost the same except the variation range. Under neutral conditions, the total atomic charge of O16 decreases with the bond breaking of O16–H18 and then increases with the bond creation of C5–O16 bond [9]. However, this is not the case in the hydrolytic deamination

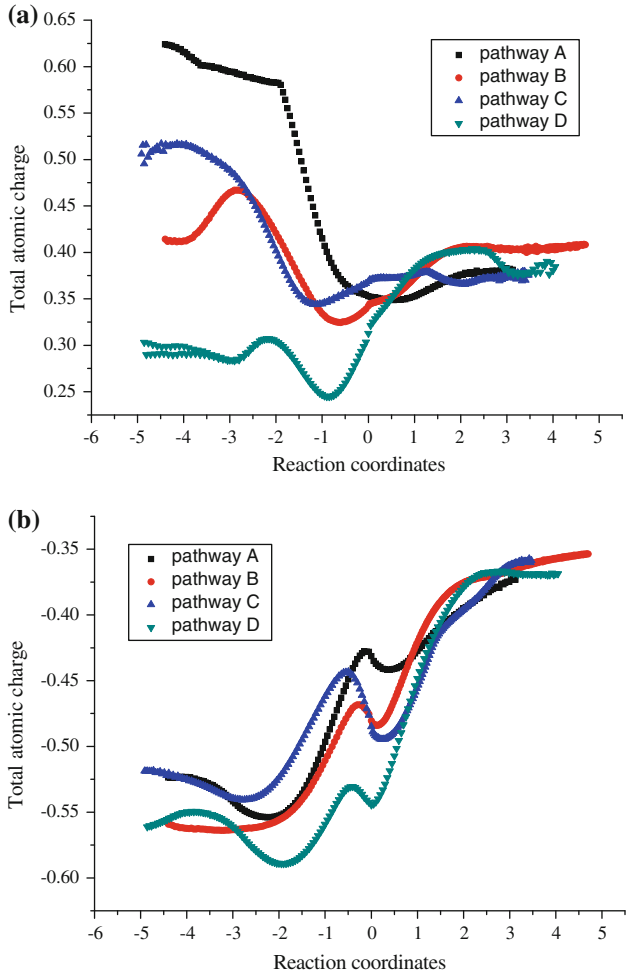

Fig. 8 Evolution of the total atomic charges on C5 (**a**) and O16 (**b**) along the reaction coordinates

of the protonated adenine. The charge variation tendency of O16 under protic circumstances firstly increases with the approaching of O16 to C5, then decreases with the cleavage of O16–H18 bond, finally increases with the C5–O16 bond formation. Pathway D is different from the other pathways. There is a crest at the reactant region. O16 forms a hydrogen bond with N10 in Int1D, thus with the approaching of O16 atom to C5 atom, the hydrogen bond O16…H10…N10 is broken, which further causes the decreasing of O16 charge.

4 Conclusions

The hydrolytic deamination of adenine in protic medium has been studied using density functional method, and four pathways have been found according to different protonated adenine.

(1) The adenine deamination occurs more easily under acidic condition than under neutral condition. Pathway A is most possible to occur with the lowest energy barriers. In this pathway, nucleophilic attack results a tetrahedral intermediate, then the assistant water acts as a shuttle to transfer a hydrogen atom to amino group, finally the ammonia molecule is released and hypoxanthine is produced.
(2) The addition of water to C6 atom with the assistance of a second water molecule is the rate-determining step for all the four pathways, which is like the proton-catalyzed hydrolytic deamination of cytosine [5]. Our calculated activation energy of adenine for pathway A is 33.4 kcal/mol (or 139.6 kJ/mol) in solution, while the reported activation energy of cytosine is 117 kJ/mol [35]. So we can see that adenine is more difficult to deaminate compared with cytosine.
(3) Solvent effect decreases the relative free energies of stationary points, while it plays an insignificant role to the structures.
(4) Reaction force evolution indicates that the simultaneity of the first step of pathway A is worst among the four pathways. The more positive charge C5 atom has at the initial intermediate region, the lower the energy barrier is.

Acknowledgments This work was supported by Scientific Research Reward Fund for Excellent Young and Middle-Aged Scientists of Shandong Province (Grant No. 2008BS02014).

References

1. Sun X, Lee JK (2007) J Org Chem 72:6548–6555
2. Almatarneh MH, Flinn CG, Poirier RA, Sokalski WA (2006) J Phys Chem A 110:8227–8234
3. Almatarneh MH, Flinn CG, Poirier RA (2008) J Chem Inf Model 48:831–843
4. Labet V, Morell C, Grand A, Toro-Labbé A (2008) J Phys Chem A 112:11487–11494
5. Labet V, Grand A, Morell C, Cadet J, Eriksson LA (2008) Theor Chem Acc 120:429–435
6. Labet V, Morell C, Cadet J, Eriksson LA, Grand A (2009) J Phys Chem A 113:2524–2533
7. Zhang A, Yang B, Li Z (2007) J Mol Struct Theochem 819:95–101
8. Zhu C, Meng F (2009) Struct Chem 20:685–691
9. Zheng H, Meng F (2009) Struct Chem 20:943–949
10. Jordan DO (1960) The chemistry of nucleic acids. Butterworths, Washington, DC, p 65
11. Shapiro R, Klein RS (1966) Biochemistry 5:2358–2362
12. Becke AD (1988) Phys Rev A 38:3098–3100
13. Lee C, Yang W, Parr RG (1988) Phys Rev B 37:785–789
14. McLean AD, Chandler GS (1980) J Chem Phys 72:5639–5648
15. Raghavachari K, Binkley JS, Seeger R, Pople JA (1980) J Chem Phys 72:650–654
16. Toro-Labbé A (1999) J Phys Chem A 103:4398–4403
17. Rincón E, Toro-Labbé A (2007) Chem Phys Lett 438:93–98
18. Furmanchuk A, Leszczynski J (2008) J Sulfur Chem 29:401–413
19. Cappelli C, Corni S, Mennucci B, Tomasi J, Cammi R (2005) Int J Quant Chem 104:716–726
20. Adhikary A, Kumar A, Becker D, Sevilla MD (2006) J Phys Chem B 110:24171–24180
21. Cances E, Mennucci B, Tomasi J (1997) J Chem Phys 107:3032–3041
22. Rappé AK, Casewit CJ, Colwell KS, Goddard WA III, Skiff WM (1992) J Am Chem Soc 114:10024–10035
23. Baboul AG, Curtiss LA, Redfern PC (1999) J Chem Phys 110:7650–7657
24. Curtiss LA, Raghavachari K (1998) J Chem Phys 109:7764–7776
25. Pople JA, Head-Gordon M, Raghavachari K (1987) J Chem Phys 87:5968–5975
26. Head-Gordon M, Pople JA, Frisch MJ (1988) Chem Phys Lett 153:503–506
27. Tang YZ, Sun JY, Sun H, Pan YR, Wang RS (2008) Theor Chem Account 119:297–303
28. Frisch MJ, Trucks GW, Schlegel HB, Scuseria GE, Robb MA, Cheeseman JR, Montgomery JA Jr, Vreven T, Kudin KN, Burant JC, Millam JM, Iyengar SS, Tomasi J, Barone V, Mennucci B, Cossi M, Scalmani G, Rega N, Petersson GA, Nakatsuji H, Hada M, Ehara M, Toyota K, Fukuda R, Hasegawa J, Ishida M, Nakajima T, Honda Y, Kitao O, Nakai H, Klene M, Li X, Knox JE, Hratchian HP, Cross JB, Adamo C, Jaramillo J, Gomperts R, Stratmann RE, Yazyev O, Austin AJ, Cammi R, Pomelli C, Ochterski JW, Ayala PY, Morokuma K, Voth GA, Salvador P, Dannenberg JJ, Zakrzewski VG, Dapprich S, Daniels AD, Strain MC, Farkas O, Malick DK, Rabuck AD, Raghavachari K, Foresman JB, Ortiz JV, Cui Q, Baboul AG, Clifford S, Cioslowski J, Stefanov BB, Liu G, Liashenko A, Piskortz P, Komaromi I, Martin RL, Fox DJ, Keith T, Al-Laham MA, Peng CY, Nanayakkara A, Challacombe M, Gill PMW, Johnson B, Chen W, Wong MW, Gonzalez C, Pople JA (2004) Gaussian 03, revision D.01. Gaussian Inc, Wallingford, CT
29. Mirkin SM (1995) Annu Rev Biophys Biomol Struct 24:319–350
30. Wu R, McMahon TB (2007) J Am Chem Soc 129:569–580
31. Fuentes-Cabrera M, Sumpter BG, Šponer JE, Šponer J, Petit L, Wells JC (2007) J Phys Chem B 111:870–879
32. Liu H, Gauld JW (2008) J Phys Chem B 112:16874–16882
33. Close DM, Crespo-Hernández CE, Gorb L, Leszczynski J (2008) J Phys Chem A 112:12702–12706
34. Sousa SF, Fernandes PA, Ramos MJ (2007) J Phys Chem A 111:10439–10452
35. Lindahl T, Nyberg B (1974) Biochemistry 13:3405–3410